water

MDPI

Article

Long-Term VOC Transport in a Thick Heterogeneous Vadose Zone and Perched Aquifers: Jerusalem Mountains Industrial Site

Ohad Shalom [1,*], Ovadia Lev [2], Matania J. Caspi [3] and Haim Gvirtzman [1]

[1] The Fredy and Nadine Herrmann Institute of Earth Sciences, The Hebrew University of Jerusalem, Jerusalem 9190401, Israel; haim.gvirtzman@mail.huji.ac.il
[2] The Institute of Chemistry, The Hebrew University of Jerusalem, Jerusalem 9190401, Israel; ovadia@mail.huji.ac.il
[3] Environmental Services Company, Neot Hovav—Eco-Industrial Park in the Negev, Be'er Sheva 84156, Israel; matic@escil.co.il
* Correspondence: ohad.shalom@mail.huji.ac.il

Abstract

Volatile organic compounds (VOCs) from historical industrial activities can persist for decades, contaminating groundwater and the unsaturated zone, yet their transport through thick, heterogeneous vadose zones is poorly understood. This study reconstructs long-term migration of tetrachloroethylene (PCE) from a former industrial site in the Jerusalem Mountains, where leakage likely began ten years after plant commissioning and systematic monitoring started decades later. A three-dimensional numerical model of flow and transport was applied, incorporating calibrated hydraulic parameters, karstic conduits, and multiphase VOC processes including advection, dispersion, phase partitioning, volatilization, and first-order degradation kinetics. Multiple model runs explored plausible leakage scenarios under sparse historical data. Simulated PCE concentrations reproduce measurements in the vadose zone (R^2 = 0.89) and deep regional aquifer (~20% normalized relative error). Results reveal pronounced preferential flows horizontally through perched aquifers and vertically along discrete faults, amplified by karstic networks. The upper vadose zone remains a persistent source, sustaining gas-phase emissions toward nearby residential areas unless targeted remediation is applied. Integrated modeling, even with limited monitoring, quantitatively reconstructs complex contaminant dynamics across saturated and unsaturated compartments, providing critical guidance for remediation. Protecting groundwater and human health requires addressing both vadose and saturated zones to prevent prolonged environmental and exposure risks.

Keywords: tetrachloroethylene; VOC transport; vadose zone modeling; karstic flow; groundwater contamination; preferential flow; remediation planning

Check for updates

Academic Editor: Zbigniew Kabala

Received: 4 February 2026
Revised: 3 March 2026
Accepted: 12 March 2026
Published: 17 March 2026

Copyright: © 2026 by the authors. Licensee MDPI, Basel, Switzerland. This article is an open access article distributed under the terms and conditions of the Creative Commons Attribution (CC BY) license.

1. Introduction

Background and Objectives

Volatile organic compounds (VOCs) have caused widespread and persistent groundwater contamination worldwide, with substantial environmental and economic consequences since the 1970s [1,2]. Many VOCs are hydrophobic and toxic, and several, particularly chlorinated solvents, are known or suspected carcinogens [3]. Releases commonly originate from industrial facilities, storage tanks, pipelines, and landfills, often resulting in long-lived contaminant sources. Once released, VOCs may persist for decades in the

subsurface due to limited sorption, slow degradation rates, and the formation of non-aqueous phase liquids (NAPLs), which sustain dissolved and vapor-phase contamination over extended periods [4].

Accurate prediction of VOC migration requires integration of transport and transformation processes across both unsaturated (vadose) and saturated zones, including advective and dispersive transport in water, diffusive and advective transport in the gas phase, phase partitioning among aqueous, gaseous, and solid phases, and degradation reactions [5] (Figure 1A). Thick vadose zones can retain and slowly transport contaminants over long periods, making them critical controls on plume evolution. Vadose-zone transport is inherently complex due to partial saturation, transient recharge, and pronounced spatial heterogeneity, which together challenge conceptualization and numerical representation.

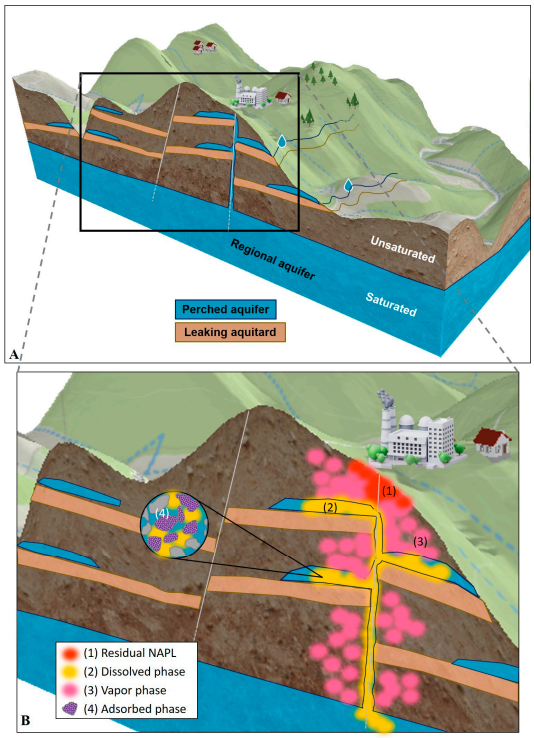


Figure 1. (**A**) A water flow scheme through a thick heterogeneous vadose zone [6]. (**B**) An enlargement demonstrating VOC transport in the vadose zone. Organic contaminants exist in 4 phases: NAPL, dissolved in water, vapor in pore-gas, and adsorbed on solid.

Several unresolved challenges continue to limit reliable numerical modeling under such conditions. Simplified approaches often approximate downward migration using average recharge rates and plug-flow concepts, yet field observations show that infiltration is spatially and temporally variable. Preferential flow processes, in which water and solutes bypass portions of the porous matrix, are common and may dominate contaminant transport [7]. Geological heterogeneity, stratification, and structural features exert strong controls on flow paths and travel times, while fractured and karstic networks can increase effective flow velocities by orders of magnitude relative to the surrounding matrix [8].

Beyond physical complexities, one major challenge is the severe lack of monitoring data during the active contamination period. In many cases, contaminant release and migration proceed unnoticed for decades, and systematic monitoring begins only after impacts are detected in groundwater. Numerical models must therefore often be constructed and evaluated using sparse, temporally limited datasets, reflecting the practical conditions at many contaminated sites.

Field-informed studies that integrate the full source-to-receptor sequence, from historical VOC source through thick vadose zones into perched and regional aquifers, remain relatively scarce. Large-scale investigations at Savannah River, Hanford, and Runcorn Peninsula have provided valuable insights into vadose-zone behavior [9–12], yet gaps remain in comprehensive three-dimensional studies combining long-term observations with coupled modeling under limited historical data [5].

Modeling the remediation outcome and transport of chlorinated solvents such as tetrachloroethylene (PCE), the focus of this study, is especially challenging because PCE migration is influenced by groundwater flow, hydrodynamic dispersion, reversible sorption, volatilization, and degradation (Figure 1B). Reductive dechlorination occurs when reducing saturated environments [13], while transformation in oxic vadose zones is limited and hydrolysis is extremely slow (half-lives > 1000 years) [14]. PCE's high volatility (Henry's constant $\approx 1.8 \times 10^{-2}$ atm·m^3·mol^{-1}) enables gas-phase transport that can either attenuate groundwater impacts or accelerate arrival at the water table via downward vapor migration [15,16]. Gas-phase transport is driven by diffusion, pressure, and temperature gradients [17,18].

Advances in numerical modeling allow three-dimensional simulation of coupled flow and transport across unsaturated and saturated zones, incorporating multiphase partitioning, volatilization, dissolution, and first-order reactions [5,19]. Representing vadose and saturated zones as a single, continuous domain facilitates explicit treatment of contaminant exchange between phases and hydrogeologic units [20]. These models, when combined with recent monitoring data and physically based assumptions, can reconstruct long-term plume evolution even under severe data scarcity.

In this study, we present a three-dimensional numerical reconstruction of long-term PCE transport from a historical industrial source through a thick, heterogeneous vadose zone containing two perched aquifers and an underlying regional aquifer in the Jerusalem Mountains. Contamination developed over decades without systematic monitoring; therefore, the transport model is constructed using limited recent monitoring data together with a previously calibrated groundwater flow model [6].

The objectives of this study are:

1. To reconstruct the long-term evolution of a PCE plume through a thick, heterogeneous vadose zone and underlying aquifers using a physically based, three-dimensional model.
2. To evaluate how vadose-zone processes, preferential flow, and karstic features control plume development and source persistence under extreme historical data scarcity.
3. To demonstrate that recent monitoring data, combined with a calibrated groundwater flow model, can plausibly inform transport simulations and support remediation planning.
4. To assess the impact of source removal on plume persistence and to delineate potential future exposure zones in adjacent residential areas.

2. Hydrogeological Setting

2.1. Studied Area

The study area is located on the mountain ridge between the Rephaim and Sorek streams in southwest Jerusalem (Figure 2A,B). For detailed geographic and geological information, see [6]. The site comprises a large-scale, stratified, folded, faulted, and karstic vadose zone overlying two perched aquifers and the deep Yarkon-Taninim regional aquifer. The vadose zone exhibits pronounced preferential flow: horizontally within perched aquifers and vertically along discrete faults, with karstic features further enhancing connectivity.

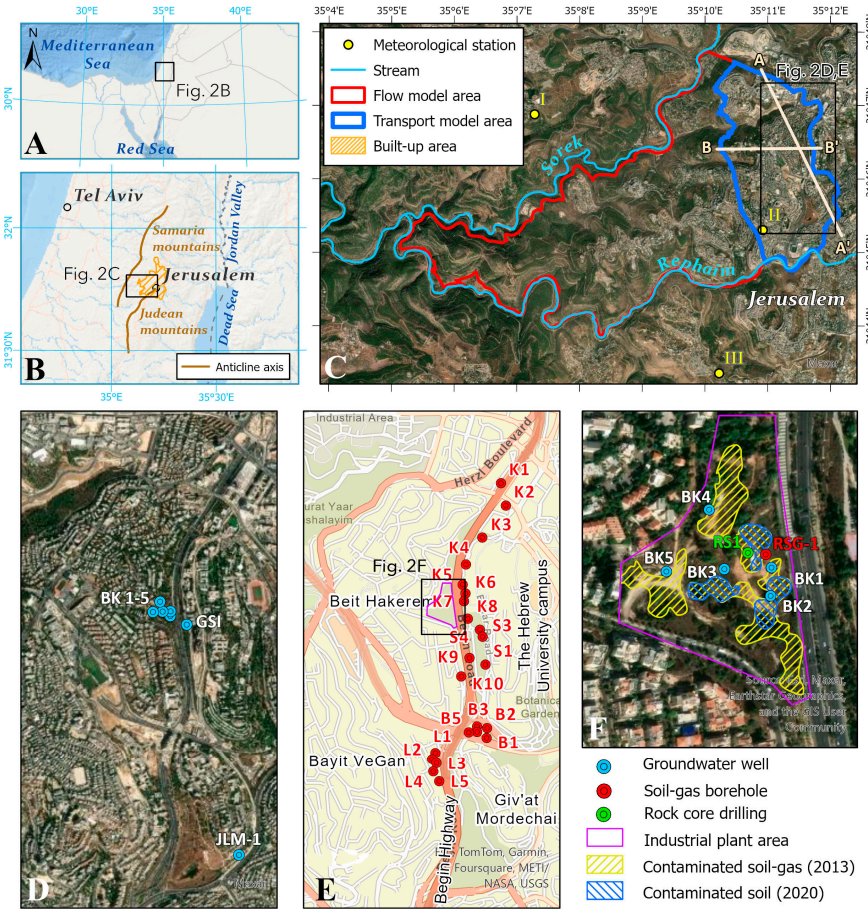


Figure 2. (**A**,**B**) are location maps of the studied area; (**C**) is an aerial photo of southwest Jerusalem and the mountain ridge between the two dry streams. The locations of three rain gauges (I. Tzuba, II. Malcha, III. Har Gilo) of the Israel Meteorological Service are shown, as well as the locations of two cross-sections shown in Figures 4 and 5. (**D**) and (**E**) are an aerial photo and a map, respectively, showing groundwater wells (blue symbols in frame (**D**)) and soil gas boreholes (red symbols in frame (**E**)) (based on [21]). (**F**) shows the contaminated spots detected in 2013 and 2020 (based on [22]).

The current modeling focuses on a 10 km^2 area in the eastern ridge (Figure 2C), encompassing the former industrial plant (~18 acres) east of the Beit Hakerem neighborhood, west of the Hebrew University Givat Ram campus, and north of Givat Mordechai neighborhood (Figure 2D,E). The main contaminant plume migrated predominantly beneath the Begin Highway. The regional aquifer lies ~300 m below ground, with multiple active wells along the ridge edges and within the study area (Supplementary Section A, Figure S1). This hydrogeological framework supports reconstruction of long-term contaminant transport under limited monitoring conditions.

2.2. Contamination History, Monitoring and Remediation

The Netz industrial site at Beit Hakerem operated from 1951 to 1997 under Israel Military Industries. The facility produced a variety of metal products, including ammunition casings and precision components, which required extensive use of chlorinated solvents, particularly tetrachloroethylene (PCE). Over the decades, PCE residues were buried or stored on-site, and leaks eventually led to the formation of a persistent subsurface contamination plume. As the solvent migrated through the subsurface, it generated degradation products such as trichloroethylene (TCE), cis-1,2-dichloroethylene (cDCE), and vinyl chloride, further complicating the contamination profile and posing risks to the vadose zone, perched aquifers, and the underlying regional aquifer. Although TCE, cDCE,

and vinyl chloride were detected historically, systematic monitoring data are available only for PCE. The absence of consistent temporal and spatial datasets for daughter products precludes reliable calibration of sequential dechlorination pathways. Therefore, reactive transport simulations focused exclusively on PCE as the primary contaminant.

Contamination was first detected in 1997 at the Jerusalem-1 (JLM 1) well (Figure 2D), located approximately 1.7 km south of the plant in the regional aquifer at a depth of ~300 m. Following this discovery, multiple monitoring campaigns documented contaminant occurrence in soil, soil gas, perched aquifers, and the regional aquifer. Major site investigations conducted in 2013 and 2020 identified numerous contaminated locations both within the plant area and in adjacent zones (Figure 2F). These datasets, together with additional borehole drilling, soil-gas surveys, and measurements of PCE adsorbed onto vadose-zone rock cores, constitute the primary observational basis for the transport modeling.

In parallel with site investigations, remediation efforts were initiated to remove contaminated surface soils and reduce ongoing contaminant loading to the subsurface. During the first remediation phase (1998–2000), shallow contaminated hotspots were identified across the industrial site, and approximately 4450 tons of soil were excavated from 27 locations (Supplementary Material, Figure S3). Subsequent monitoring revealed that residual contamination remained in several areas. Consequently, a second remediation phase was conducted in 2020, during which contaminated soil was excavated [23] to depths of up to 8 m in remaining hotspots (Figure 2F; Supplementary Materials, Figure S6).

Systematic monitoring of the site began only decades after the onset of contamination, resulting in limited temporal coverage of plume development. The available datasets primarily represent conditions over the past 10–25 years, long after initial releases occurred. While key findings and representative survey results are presented in Figures S2–S6 (Supplementary Section A), the complete chronological sequence of monitoring and remediation phases, including borehole locations, sampling depths, and analytical results, is detailed in Supplementary Section B.

The prolonged contamination history, delayed detection, evolving monitoring efforts, and partial source removal collectively underscore the complexity of reconstructing plume evolution at the site. The modeling framework presented in this study integrates these limited observational datasets with a calibrated groundwater flow model to simulate long-term PCE transport from the vadose zone, through perched aquifers, and into the regional aquifer, while accounting for the effects of remediation on source persistence and plume behavior.

3. Methods

3.1. Model Framework and Discretization

A three-dimensional finite-element groundwater flow and solute transport model was developed for the Jerusalem Mountains vadose zone using the FEFLOW (7.3) software package [24]. The numerical domain represents the eastern portion of the mountain ridge and includes the thick unsaturated zone, the two perched aquifers, and the upper part of the regional Yarkon–Taninim aquifer. The computational mesh (Figure 3) consists of 40 vertical layers and 599,620 elements, with a mean element diameter of approximately 36 m. Vertical discretization follows the lithological formations to preserve stratigraphic continuity, while horizontal refinement was applied in the vicinity of major faults in order to capture steep hydraulic gradients and preferential flow features.

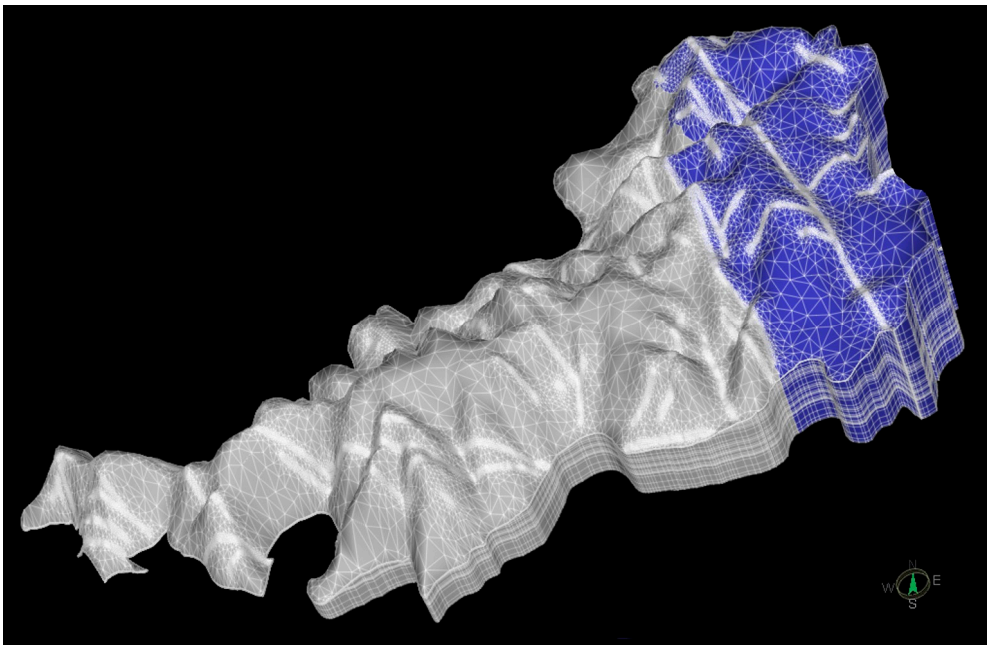


Figure 3. The 3D mesh of the modeling domain. The whole domain was used for the flow simulations [6], and the blue-colored one is used in the current study for the transport simulations. Note the large north–south fault in the center of the modeled area.

The simulation period extends from 1950 to 2024, corresponding to the estimated onset of industrial activity and the most recent monitoring data. A maximum time step of one day was used to match the temporal resolution of the rainfall record, with automatic time-step adjustment applied to ensure numerical stability during transient recharge events.

Preferential flow through karstic conduits within the carbonate formations of the Judea Group was explicitly represented in the model. Based on regional field observations and previous studies of karst morphology in the Jerusalem Mountains [25,26], conduits were parameterized using an average spacing of 150 m, a typical length of 80 m, and an effective hydraulic aperture of 0.001 m, corresponding to a representative cross-sectional area of 0.01 m^2.

It is important to note that these parameters do not aim to represent site-specific mapped karst features, for which direct data are unavailable. Instead, they provide an effective representation of preferential flow at the model scale. In such representations, conduit spacing and hydraulic aperture exert opposing controls on vertical fluxes: decreasing spacing increases connectivity, whereas increasing aperture enhances transmissivity. Consequently, the transport dynamics are primarily governed by the combined (effective) influence of these parameters rather than by their individual absolute values.

This effective karst parameterization was previously calibrated against high-resolution measured hydrographs in the same hydrogeological setting [6], providing independent support for the adopted conduit density–aperture combination. The resulting representation reproduces the observed acceleration of vertical flow and solute transport relative to matrix flow by approximately 2–3 orders of magnitude, consistent with regional-scale karst behavior in the Judea Group.

3.2. Boundary Conditions and Transport Parameters

The flow boundary conditions were adapted from the previously calibrated regional-scale groundwater flow model [6] and adjusted to reflect the reduced spatial extent of the present transport domain. The northern, eastern, and southern model boundaries coincide with hydrogeologic flow divides or zones of negligible lateral flow identified in the regional flow field. The western boundary corresponds to a major fractured zone separating the eastern and western portions of the ridge, along which horizontal groundwater exchange is minimal. Flow in both perched aquifers is predominantly oriented southward, and unsaturated-zone flow is largely vertical. Accordingly, this boundary was treated as a no-flow boundary for both saturated and unsaturated conditions, providing a hydraulically justified truncation of the original larger model domain.

At the upper boundary, transient recharge was applied using a daily rainfall record spanning 1951–2024, constructed from the average of three nearby meteorological stations (Figure 2C; Supplementary Section A, Figure S7). Recharge was calculated as a fraction of precipitation, following land-use-dependent infiltration coefficients established in the flow model calibration [6]. During the industrial operation period (1951–1997), recharge across the plant site was set to 17% of rainfall, consistent with urbanized surface conditions. Following demolition of the facility and site opening in the late 1990s, recharge increased to 38%, representative of open-field conditions.

At the lower boundary of the vadose domain, a gravity-driven unit hydraulic gradient was imposed to represent long-term downward percolation toward the regional aquifer. This formulation reflects predominantly gravity-controlled flow under aerated conditions and constitutes a simplified representation of deep drainage. The model solves variably saturated flow; therefore, the position of the saturated–unsaturated interface evolves dynamically within the domain rather than being prescribed as a fixed water table.

A major north–south fault bisects the modeled area (Figure 3). The eastern block is hydraulically connected to the regional groundwater system, whereas the western block remains largely unsaturated. Accordingly, prescribed hydraulic heads based on measured groundwater levels were applied along the saturated eastern sector, including the vicinity of well JLM-1. In contrast, vertical gravity-driven drainage dominates beneath the unsaturated western sector.

Although simulations include years preceding the cessation of pumping at well JLM-1 in the 1990s, reconstructed contaminant timelines indicate that PCE had not yet reached the regional aquifer during the active abstraction period. Therefore, transient pumping-induced drawdown was not explicitly modeled, and its influence on long-term contaminant flux to the regional aquifer is expected to be limited. The PCE source was represented at the top of the domain in areas identified as historically contaminated based on soil excavation campaigns and hotspot mapping (Figure 2F; Supplementary Section A, Figures S4–S6). Industrial activities involved extensive use of tetrachloroethylene, with solvent residues buried in barrels within the plant yard [27]. Corrosion and leakage over time resulted in the formation of dense non-aqueous phase liquid (DNAPL) in the shallow subsurface. The representation of DNAPL as a constant solubility boundary condition constitutes a simplified conceptualization of source behavior. In fractured and karstified carbonate environments, DNAPL architecture is expected to be spatially heterogeneous and potentially controlled by structural discontinuities. Field investigations at the site indicate limited evidence of deep DNAPL accumulation within the ~300 m thick vadose zone; however, small and persistent DNAPL pools at depth cannot be entirely excluded. The adopted approach may overestimate DNAPL presence near the source zone while underrepresenting localized accumulations at depth. Given the limited subsurface constraints, the objective is not to resolve detailed DNAPL architecture, but to simulate a sustained dissolution source com-

patible with observed concentration patterns. The modeled configuration should therefore be interpreted as a plausible scenario rather than a uniquely constrained reconstruction.

As direct information on the timing and spatial distribution of leakage is unavailable, the onset of contamination was assumed to occur in 1960, approximately ten years after plant operations began. This timing is consistent with preliminary transport calculations required to reproduce the observed arrival of contamination in the regional aquifer during the 1990s. The assumed leakage onset in 1960 was determined through iterative calibration. Multiple simulations were performed using alternative release initiation years and varying source strengths in a trial-and-error framework to evaluate their influence on plume evolution and agreement with observed concentration data.

Results indicate that, due to the multi-decadal residence times within the vadose zone and perched aquifers, moderate variations in the assumed start time primarily influence early-stage plume development but exert limited control on present-day plume geometry. The selected onset year provided the best overall agreement with the spatial distribution and magnitude of measured concentrations. It should be emphasized that the objective is not to reconstruct the historical leakage chronology with absolute certainty, but to identify a physically consistent scenario that reconciles the limited monitoring data with the hydrogeological framework. The selected onset year therefore represents a plausible reconstruction rather than a uniquely constrained historical determination.

Rainwater infiltrating through contaminated soil was assumed to become saturated with PCE, and the source zone was therefore implemented using a constant solubility concentration boundary corresponding to the maximum aqueous solubility of PCE at 20 °C (160,000 μg/L). The contamination source in the shallow subsurface, consisting of NAPL-saturated soil, remained active from the initial leakage in 1960 until the complete excavation of contaminated soil in 2020. The source area decreased from 19 to 9 dunams after the first phase of soil removal in 2000. This formulation accounts for the heterogeneous DNAPL architecture, including blobs, ganglia, and small pools, without requiring explicit representation of individual DNAPL bodies. Field observations from soil excavations and recent rock coring indicate that the majority of DNAPL is confined to the upper 10 m of the subsurface, with only sporadic occurrences detected at greater depths (up to approximately 50 m). Given the limited extent of deeper DNAPL and the high solubility of PCE, downward migration of DNAPL was considered negligible relative to dissolved-phase transport.

PCE transport was simulated as a multi-process system including advection, hydrodynamic dispersion, phase partitioning between water, gas, and solid phases, volatilization, and first-order degradation. PCE degradation was represented using first-order kinetics. Based on reported hydrolysis rates for haloalkenes [14], a half-life exceeding 1000 years was assumed, corresponding to a very small first-order rate constant (k). Hydrogeological characterization indicates predominantly oxic conditions throughout the vadose zone, including the perched aquifer. Under such oxidizing conditions, reductive dechlorination is expected to be limited [5], and degradation is therefore assumed to be slow and primarily abiotic. In the absence of site-specific geochemical evidence supporting spatial variability in redox conditions, the first-order rate constant was applied uniformly across both unsaturated and saturated zones. Parameter values for Henry's law constant (temperature dependent), solid–water partitioning coefficients (expressed as Kd), dispersivities, and air–water mass-transfer relationships. A complete list of parameter values, units, references, and assumptions for different hydrogeologic units is provided in Supplementary Section C.

Model evaluation relied on available monitoring data from the perched aquifers, the regional aquifer, soil-gas surveys, and VOC concentrations adsorbed to rock material within the vadose zone. These datasets span the last 10–25 years and represent the only direct observational constraints on plume evolution. A chronological summary of all monitoring phases, sampling efforts, and major findings is presented in Supplementary Section B.

Together, the coupled flow and transport model integrates vadose-zone and groundwater processes within a single three-dimensional framework, explicitly accounting for preferential flow through faults and karstic conduits and enabling reconstruction of long-term PCE plume development under conditions of pronounced geological complexity and severe historical data limitations.

4. Results and Discussion

4.1. Groundwater Flow System and Vadose-Zone Dynamics

The calibrated flow model of the Jerusalem Mountains site provides the hydrodynamic framework for simulating PCE transport [6]. The modeled system consists of two perched aquifers, their intervening aquitards, and a deep regional aquifer (Yarkon-Taninim). Vertical percolation dominates in the unsaturated zone, with horizontal flow concentrated within the saturated lenses of the perched aquifers and the regional aquifer.

The vadose zone exhibits a wide range of moisture contents. Away from perched aquifers and faults, water saturation varies between 10 and 50%, reflecting predominantly unsaturated flow conditions. Beneath the perched aquifers and along vertical faults, saturation locally increases to 50–80%, forming preferential pathways for rapid vertical flow. The capillary fringe, immediately above the water table, reaches 80–90% saturation.

Hydraulic gradients drive horizontal flow in the saturated aquifers with typical velocities of 0.01–0.2 m/day. In contrast, vertical velocities in the aquitards are generally below 0.001 m/day, representing slow leakage to underlying units. Flow through karstic conduits in the limestone formations is 2–3 orders of magnitude faster than in the surrounding matrix, reflecting their importance in connecting perched and deep aquifers. In the unsaturated zone, vertical flow velocities average ~0.005 m/day, except along faults where flow can reach ~0.05 m/day; notably, faults account for approximately one-third of the total vertical flux.

The combined saturated thickness of the perched aquifers reaches up to 25 m, highlighting their role as transient reservoirs. Groundwater accumulation occurs preferentially in local synclines and low-lying zones adjacent to faults. The spatial distribution of flow vectors indicates three dominant discharge routes from the perched aquifers: (i) vertical leakage through aquitards, (ii) vertical flow along discrete faults, and (iii) lateral emergence via springs. Among these, vertical leakage and fault-mediated flow are the main pathways controlling contaminant migration to the regional aquifer.

Figures 4 and 5 show cross-sectional distributions of hydrostratigraphy, saturation degree, and flow velocity vectors along and across the plume's primary direction of spread. Figure 6 presents horizontal maps of saturation and velocity in the perched aquifers, highlighting areas of convergence and preferential flow. These results establish the hydrodynamic context for interpreting PCE transport in the subsequent sections.

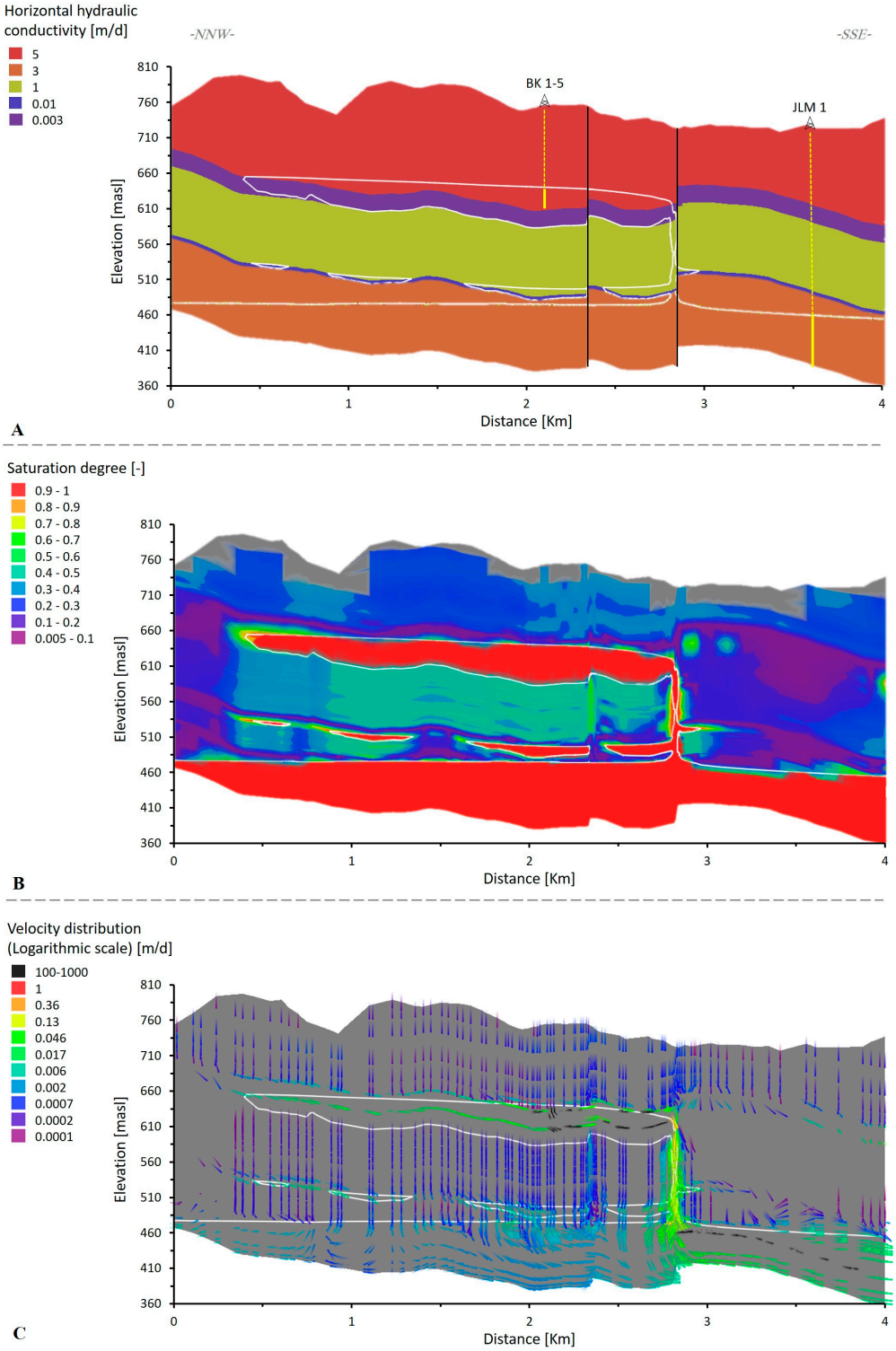


Figure 4. Modeling results on cross-section A-A' whose location is shown in Figure 2C. Results include (**A**) hydrostratigraphy with well locations (in yellow), (**B**) saturation degree and (**C**) velocity distribution. White lines mark atmospheric pressure, surrounding saturated water lenses.

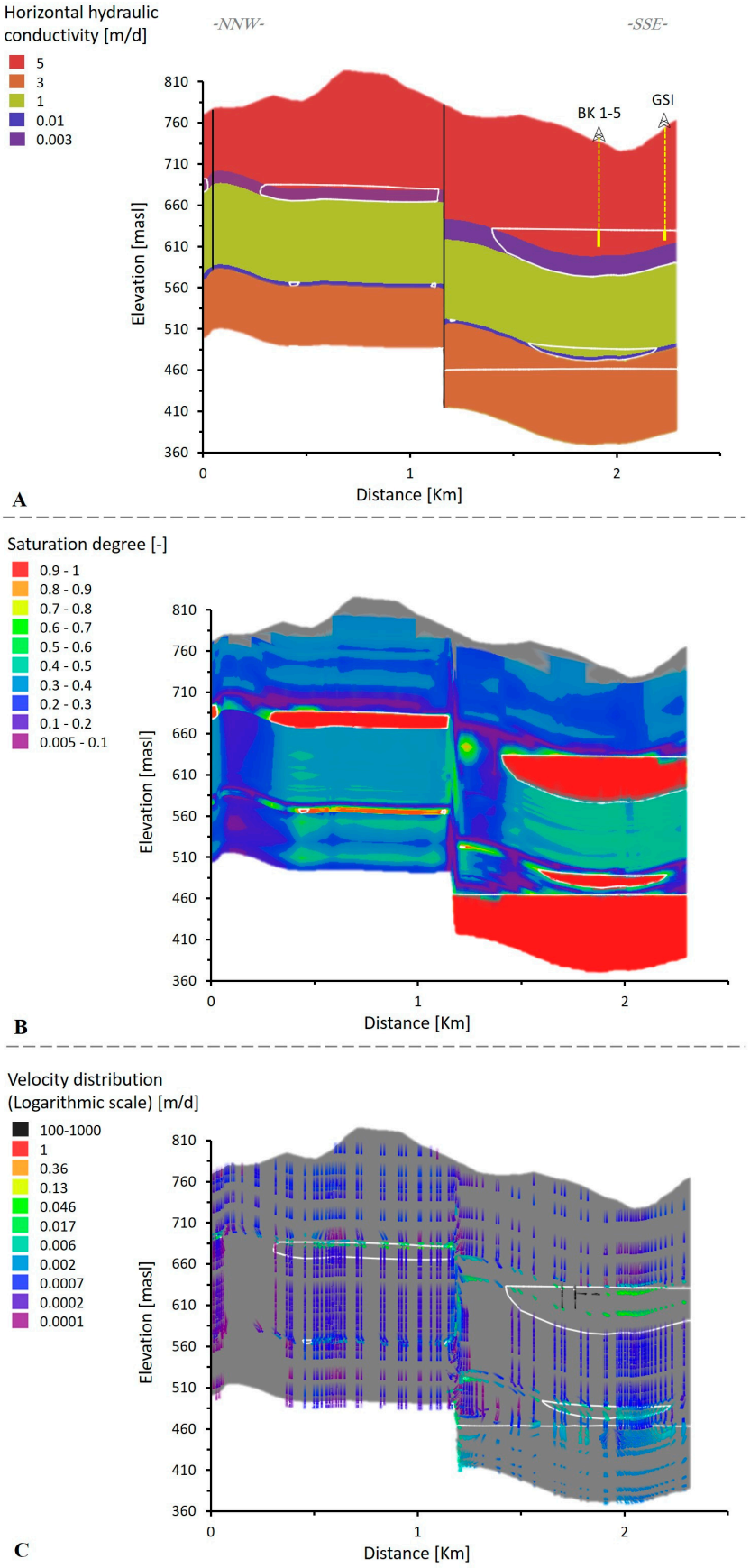


Figure 5. Modeling results on cross-section B-B′ whose location is shown in Figure 2C. Results include (**A**) hydrostratigraphy with well locations (in yellow), (**B**) saturation degree and (**C**) velocity distribution. White lines mark atmospheric pressure, surrounding saturated water lenses.

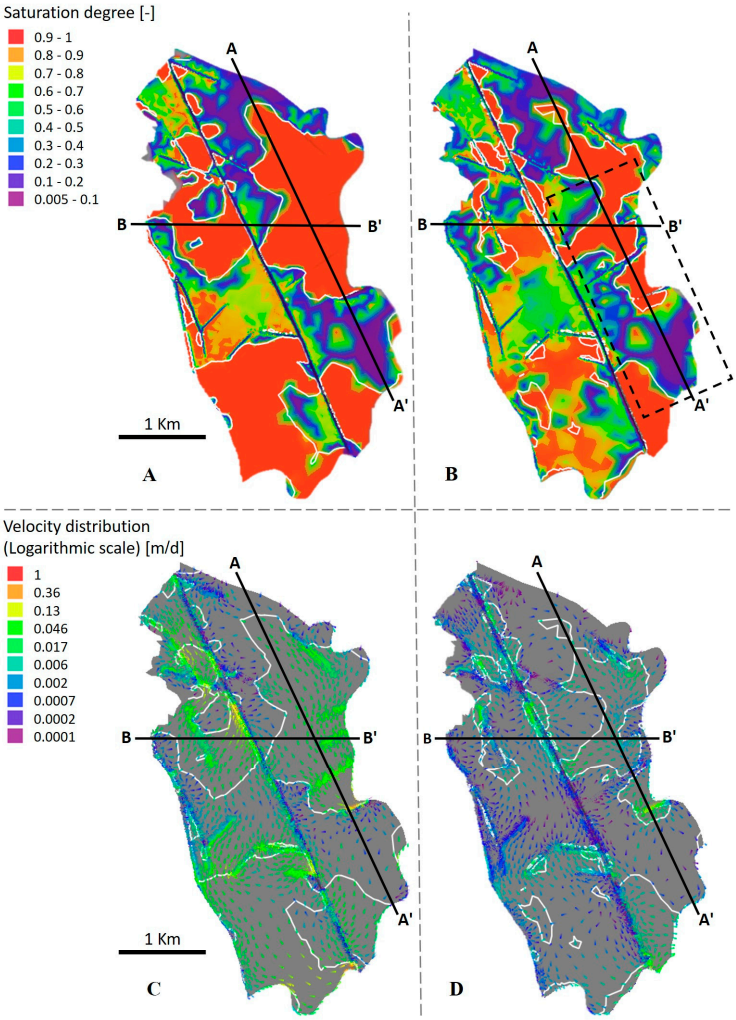


Figure 6. Water saturation degree maps of (**A**) upper and (**B**) lower perched aquifers and velocity distribution maps of (**C**) upper and (**D**) lower perched aquifers. The locations of the two cross-sections shown in Figures 4 and 5 are marked. The location of the images shown in Figure 8 are marked by a dashed rectangle in (**B**).

4.2. Reactive Transport Modeling

The reactive transport modeling focuses exclusively on PCE, as it represents the primary contaminant and the single compound consistently monitored in all relevant phases: dissolved in groundwater, as vapor in soil pores, and adsorbed in rock cores. Reconstructing the transient migration of PCE from its initial release was challenging due to the long delay between the start of plant operations and the commencement of systematic monitoring. Limited historical data were available for the perched and regional aquifers, and early vadose-zone conditions remain largely unknown. To address these uncertainties, multiple model runs were performed using the calibrated dispersivity values and the karstic conduit network to explore plausible leakage scenarios and source distributions. The scenario presented here assumes that leakage began approximately ten years after the plant started operating (1960). This simulation provided the best agreement with measured concentrations across the vadose zone, perched aquifers, and regional aquifer.

PCE transport in the vadose zone is predominantly vertical, with locally accelerated flow along discrete faults and karstic conduits. Horizontal spreading occurs mainly within the perched aquifers, which, despite their limited lateral extent, act as temporary storage zones and strongly influence the timing and magnitude of plume arrival to the regional aquifer. The buffering capacity of the perched aquifers can be quantified using previously

derived flow velocities and residence times for the same structural framework [6]. Simulated velocities indicate that vertical leakage through aquitards occurs at <0.001 m/day, whereas preferential flow along faults may be one to two orders of magnitude faster. Under matrix-dominated conditions, groundwater requires approximately 50 years to reach the upper perched aquifer and an additional 50 years to reach the lower aquifer, followed by 5–10 years for lateral drainage. Total travel times from infiltration to discharge range between 50 and 150 years. These estimates demonstrate that perched aquifers function as temporary storage reservoirs, substantially delaying contaminant migration compared to rapid fault-controlled pathways.

The simulations indicate (Figures 7 and 8) that five years after leakage began (1965), PCE migrated vertically through the upper unsaturated zone, partially via the karstic network, with only ~0.1% of the source concentration reaching the water table of the upper perched aquifer. By 1975, concentrations beneath the plant had increased to ~1%, and the plume spread horizontally along the perched aquifer flow direction. By 1985, vertical penetration into the lower unsaturated zone and the deep regional aquifer along faults was evident. Over the subsequent decades, the plume continued to expand, eventually reaching the JLM 1 pumping well. Although a unit-gradient boundary was applied beneath the vadose zone, the gravity-dominated regime and the absence of active pumping during the simulated period suggest that calculated PCE fluxes to the regional aquifer are not significantly biased by this simplification. Because vertical transport is primarily controlled by matrix permeability and structural pathways rather than by imposed hydraulic heads, the boundary condition is expected to have limited influence on long-term contaminant migration estimates. Concentrations directly beneath the plant decreased following soil excavation, while lateral migration within the aquifers persisted.

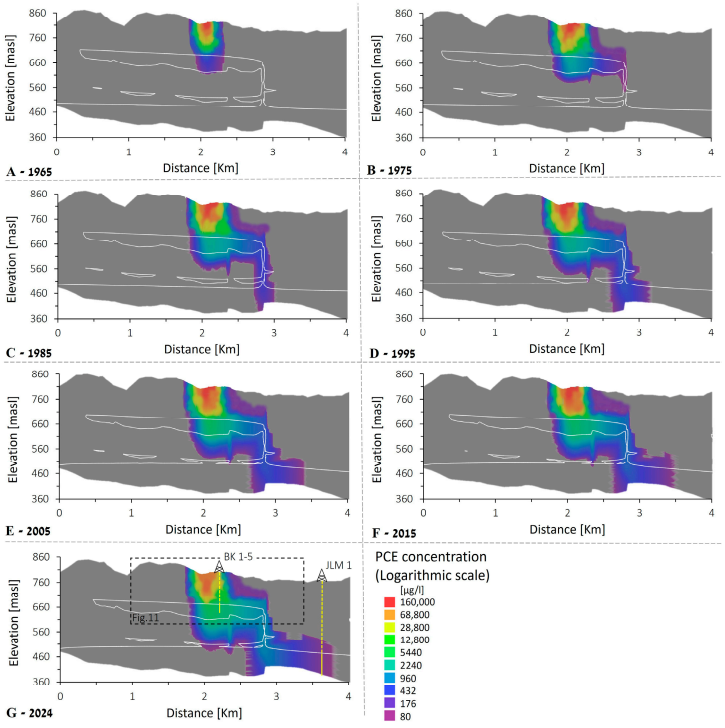


Figure 7. Modeling results of 64-year-long dissolved-PCE spreading on cross-section A-A′ (whose flow field is shown in Figure 4). Contaminants leak from the Netz site and move downward and southward through the unsaturated zone and the perched aquifers into the deep regional aquifer. Colors indicate relative concentrations using a logarithmic scale, and white lines mark atmospheric pressure and surround saturated water lenses. The rectangular area in G-2024 is enlarged in Figure 11.

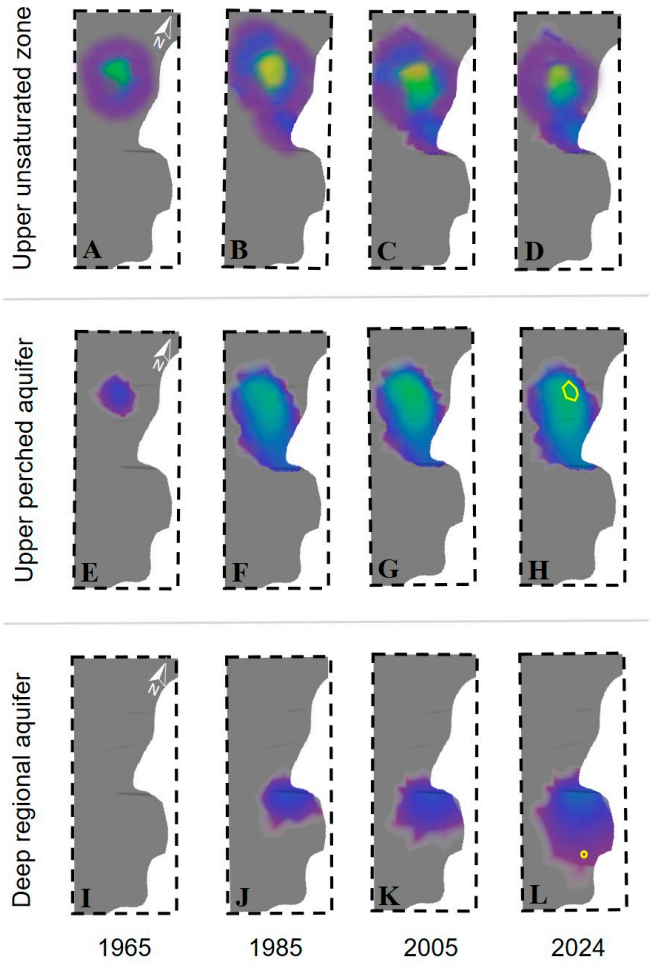


Figure 8. Modeling results of 64-year-long dissolved-PCE spreading on three horizontal sections (location shown in Figure 6B, marked by dashed rectangle) perpendicular to the cross-section shown in Figure 7. Colors indicate relative concentrations using a logarithmic scale, as in Figure 7. The wells areas used for comparison in Figures 9 and 10 are marked in yellow on (**L**) and (**H**), respectively. (**A**–**D**) illustrate the spread of contamination in the upper unsaturated zone in 1965, 1985, 2005, and 2024, respectively. For the same years, (**E**–**H**) illustrate the spread for the upper perched aquifer, and (**I**–**L**) illustrate the spread for the deep regional aquifer.

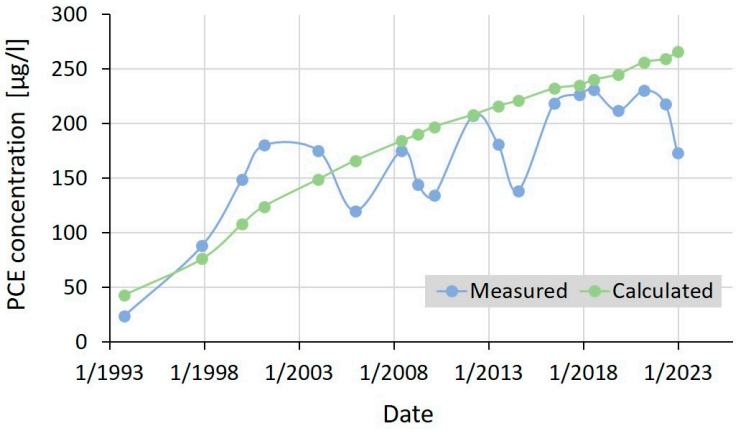


Figure 9. Comparison between simulated and measured dissolved-PCE concentrations in the regional aquifer (JLM 1 well, Figure 2D).

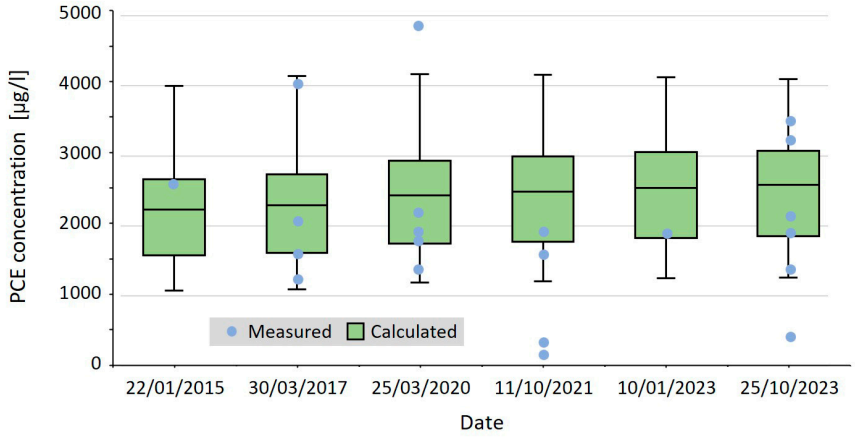


Figure 10. Comparison between simulated and measured (six boreholes, Figure 2D) dissolved-PCE concentrations in the upper perched aquifer. The range of simulated results was determined based on the model results in the wells area (marked in white in Figure 8H). The boxplots denote the median values, the standard deviations, and the upper and lower values in the range.

The simulated flow and transport fields are consistent with observed water saturation and velocity distributions, as well as with measured PCE concentrations. These results highlight the dominant mechanisms controlling plume migration: vertical advection through the unsaturated zone, horizontal transport within perched aquifers, and localized acceleration along karstic and faulted pathways. Model results indicate that plume evolution is primarily controlled by advective transport and preferential flow along structural pathways, whereas degradation plays a secondary role over the simulated time scale. Given the very long hydrolysis half-life of PCE and the predominantly oxic conditions in the vadose zone, decay rates are small relative to transport rates. Consequently, concentration patterns are governed mainly by flow architecture rather than by reactive attenuation.

It should be noted that geochemical interactions with minerals, as well as pH, alkalinity, and related factors, are not explicitly considered in the current simulations due to the lack of sufficient site-specific data. These processes may affect VOC transport and transformation, and represent an important avenue for future research in this area. Similarly, the long-term conservative versus non-conservative behavior of VOCs was not explicitly evaluated due to the limited geochemical and redox data available for the site. While such factors may affect attenuation and persistence, the present simulations focus on advective transport and first-order PCE degradation, providing a first-order assessment of long-term plume behavior. Future studies could examine these geochemical influences in more detail once sufficient site-specific measurements are available.

4.3. Comparison Between Measured and Simulated Concentrations

Simulated PCE concentrations were compared with available measurements in the vadose zone, perched aquifers, and the regional aquifer to evaluate the plausibility of the modeled transport. Monitoring data for the regional aquifer (JLM 1 well) show PCE concentrations increasing from 30 to 260 µg/L over ~30 years (1993–2024), representing approximately 0.1% of the maximum source concentration. The modeled results reproduce this trend closely, with a root mean square deviation of 37 µg/L, corresponding to ~20% normalized relative error (Figure 9).

For the upper perched aquifer, monitoring in the Beit Hakerem and GSI boreholes (2013–2023) revealed PCE concentrations ranging between 1290 and 4050 µg/L (~1–2% of the maximum source concentration). Simulated concentrations in the corresponding areas show good agreement with these measurements, capturing both the spatial distribution and the magnitude of contamination (Figure 10). The modeled horizontal spreading within

perched aquifers reflects both aquifer geometry and flow convergence, consistent with observed data.

Additional validation was performed using PCE concentrations measured as vapor in soil pores and adsorbed in rock cores. Assuming local equilibrium among aqueous, vapor, and solid phases, the measured vapor and rock-adsorbed concentrations were converted to equivalent aqueous-phase concentrations using Henry's law and the soil–water partition coefficient, respectively. Comparison with simulated values shows strong agreement (R^2 = 0.89) in the central contaminated zone (Figure 11). Boreholes located north and south of the site show very low measured concentrations (<1 μg/L), consistent with simulated predictions, confirming that contamination remains largely confined to the plant vicinity.

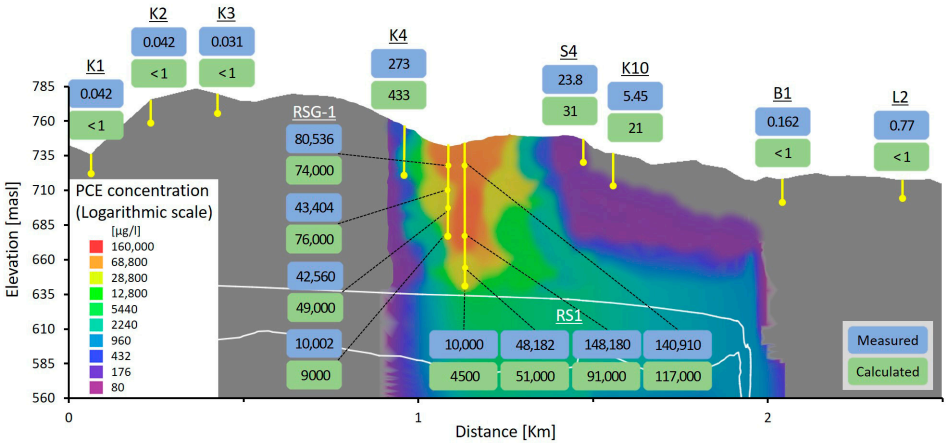


Figure 11. Comparison between simulated and measured PCE concentrations in moisture across the upper vadose zone. At each sampling point (yellow points) along the boreholes (yellow lines), two values are provided for the dissolved PCE concentration in the moisture: measured values (using the partition coefficients) and the simulated ones. Model simulated concentrations are sketched in the background as in Figure 7G, but the colored scale is in μg/L units. Borehole locations are shown in Figure 2E,F.

These comparisons demonstrate that the adopted transport model, under the assumptions of source timing, dispersivity, and karstic flow, captures the main features of PCE migration across both unsaturated and saturated zones. The model reproduces the observed plume geometry, vertical penetration through the vadose zone, lateral spreading in perched aquifers, and transport into the regional aquifer, providing a robust basis for assessing future contamination scenarios and remediation planning.

4.4. Practical Implications

The numerical simulations provide an integrated assessment of PCE distribution within the vadose zone, perched aquifers, and the deep regional aquifer, offering insight into plume evolution, long-term persistence, and implications for remediation. Although contaminated surface soils were fully excavated by 2020 and subsequent infiltration consists of uncontaminated rainfall, the model indicates continued slow release of PCE from the upper vadose zone over the coming decades. As a result, contamination persists in deeper unsaturated layers and in the underlying saturated systems, highlighting the long-term role of the vadose zone as a contaminant reservoir (Figure 12).

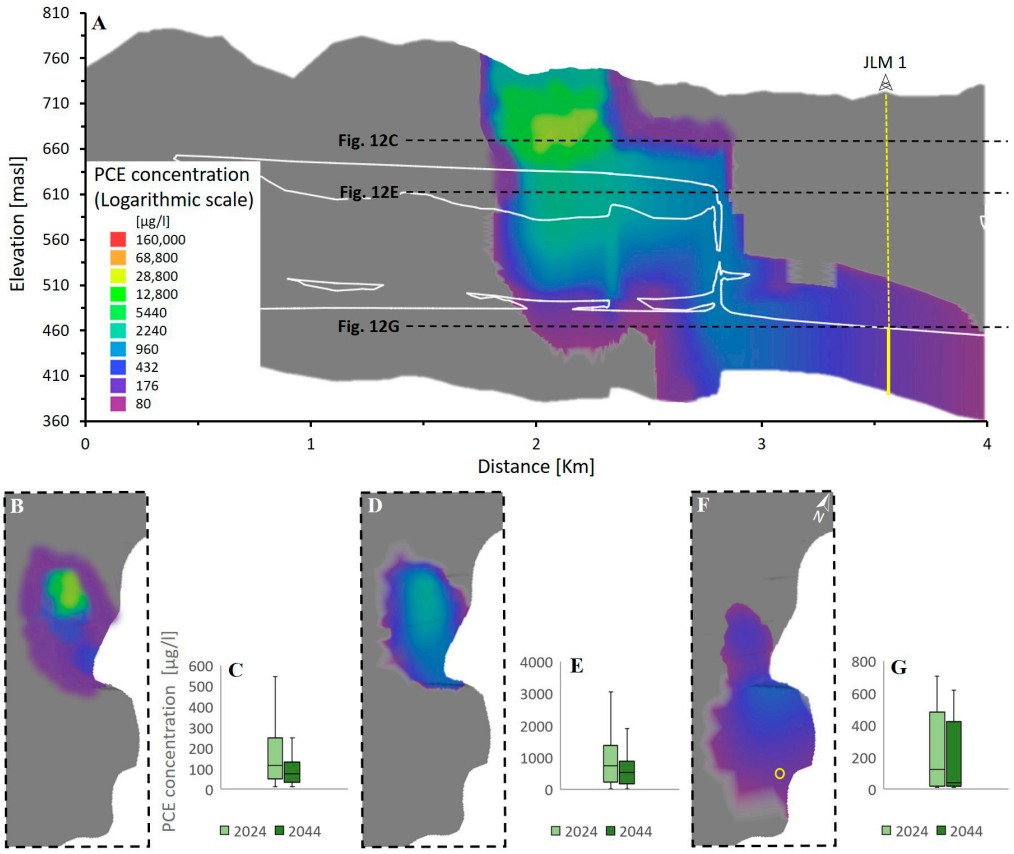


Figure 12. Predicted PCE concentrations for the year 2044 if no remedial actions are taken (**A**) across the vertical section A-A′ (whose past PCE spreading is shown in Figure 7), and in three horizontal plains (whose past PCE spreading is shown in Figure 8) perpendicular to the cross-section (marked with dashed lines on (**A**)): (**B**) upper vadose zone, (**D**) upper perched aquifer, and (**F**) deep regional aquifer. (**C**), (**E**) and (**G**) show a comparison between present and future simulated dissolved-PCE concentrations in the upper vadose zone, the upper perched aquifer, and the deep regional aquifer, respectively. The boxplots denote the median values, the standard deviations, and the upper and lower values in the range. The location of JLM 1 Well is marked on (**A**,**F**) in yellow.

Within the upper vadose zone, the plume currently extends over an area approximately fifteen times larger than the original plant footprint. Simulations predict only a limited reduction (about 10%) in this affected area over the next 20 years, with elevated concentrations remaining near the former source zone despite surface soil removal (Figure 12B,C). Continued lateral expansion is constrained by a major fault that redirects flow downward, promoting vertical migration rather than horizontal spreading. In the upper perched aquifer, PCE exhibits substantial lateral extent, with concentrations exceeding 1000 µg/L across an area roughly five times larger than the plant site. Over time, the spatial footprint is expected to gradually contract, not due to dilution, but because this section lacks a laterally continuous saturated unit, resulting in predominantly vertical flow and limited horizontal plume propagation (Figure 12D,E).

Plume evolution is governed by two dominant transport mechanisms: preferential vertical migration along discrete faults and lateral spreading within perched aquifers. Fault-controlled flow pathways were responsible for the relatively rapid historical contamination of the deep regional aquifer but are spatially localized and therefore contribute minimally to future plume expansion. In contrast, leakage from perched aquifers through underlying aquitards sustains broader contamination of saturated zones and represents the main driver of long-term plume persistence (Figure 12F). The deep regional aquifer may experience a further increase of approximately 20% in contaminated area over the next two decades;

however, concentrations are expected to remain moderated by the large groundwater volumes and associated dispersion within this extensive system (Figure 12G).

Measured PCE concentrations in groundwater locally exceed regulatory thresholds. For reference, the Israeli drinking water standard for PCE is 10 μg/L, while the U.S. maximum contaminant level (MCL) is 5 μg/L. The Israeli Tier 1 Residential Risk-Based Target Level (RBTL) for PCE vapor protective of indoor inhalation exposure is 2100 $\mu g/m^3$. Exceedances are primarily confined to the immediate vicinity of the source zone, whereas concentrations decrease substantially at greater distances.

The structural control on horizontal plume migration has important implications for potential exposure in overlying urban areas. Lateral contaminant spreading is effectively confined to zones where perched aquifers are laterally continuous. Accordingly, areas situated above the contaminated perched aquifer, particularly the margins of the Hebrew University Givat Ram campus and the southeastern portions of the Beit Hakerem neighborhood, may remain susceptible to long-term impacts associated with persistent PCE sources in the vadose zone and shallow saturated system. In contrast, other surrounding neighborhoods are unlikely to experience significant contamination over time, as plume migration is interrupted where saturated continuity is absent. Notably, the Givat Mordechai neighborhood lies south of a major fault that hydraulically disconnects it from the contaminated system, substantially reducing its vulnerability.

From a remediation standpoint, the results indicate that interventions focused solely on groundwater extraction from perched or regional aquifers are insufficient to eliminate the long-term source of contamination. The vadose zone beneath and immediately surrounding the former industrial site remains the dominant reservoir sustaining contaminant flux into the saturated system. While pumping may reduce dissolved mass in groundwater, effective long-term risk mitigation will likely require targeted vadose-zone treatments, such as additional soil removal or in situ remediation methods. At the same time, the constrained nature of horizontal plume migration provides reassurance that widespread expansion of contamination into surrounding urban areas is improbable.

Overall, these findings demonstrate the critical role of vadose-zone processes and hydrogeologic structure in controlling long-term VOC transport. Remediation strategies must therefore integrate both unsaturated and saturated compartments to effectively limit environmental impacts and human exposure. Accurate representation of vadose-zone storage and transport is essential for prioritizing intervention zones, designing remediation systems, and predicting the future spatial and temporal evolution of PCE in accordance with regulatory thresholds for groundwater and soil gas.

The persistence behavior observed at this site reflects mechanisms that are typical of thick vadose-zone systems impacted by chlorinated solvents: prolonged residence times, delayed contaminant release from intermediate storage zones, and limited natural attenuation under predominantly oxic conditions [5]. In such environments, contaminant migration is commonly controlled by matrix flow, intermediate storage within perched systems, and slow dissolution processes rather than by rapid preferential pathways alone.

However, the approximately 300-m-thick unsaturated zone at the study site represents an extreme hydrogeological configuration that amplifies these processes, resulting in particularly extended contaminant lifetimes compared to more common shallow groundwater settings [28]. Thus, while the underlying transport and attenuation mechanisms are not exceptional, their temporal scale and system-wide impact in the present case lie toward the upper range documented for thick unsaturated-zone VOC sites. This distinction is important for groundwater management: deep vadose systems may not exhibit unusual processes, but their scale can substantially prolong contaminant persistence and delay aquifer recovery [29]. The findings therefore contribute to the broader understanding of

chlorinated VOC behavior in thick unsaturated carbonate environments and highlight the need for long-term management strategies in similar hydrogeological settings worldwide.

5. Summary

This study provides a comprehensive reconstruction of long-term tetrachloroethylene (PCE) transport from a historical industrial source through the thick, heterogeneous vadose zone and underlying aquifers in the Jerusalem Mountains. Leakage likely began approximately ten years after plant operation commenced, and systematic monitoring started decades later, resulting in a poorly gauged system. Despite these limitations, the integration of long-term monitoring data with a calibrated three-dimensional flow model enabled quantitative simulation of contaminant transport and attenuation in both the unsaturated and saturated zones. The transport model reproduces measured concentrations in the vadose zone (R^2 = 0.89) and in the deep regional aquifer (~20% normalized relative error at JLM 1 well), providing a robust basis for evaluating subsurface contaminant dynamics.

The results highlight the complex hydrological behavior of the Jerusalem Mountains vadose zone, which exhibits pronounced heterogeneity and multiple preferential flow pathways. Horizontal transport occurs primarily through perched aquifers, while vertical flow along discrete faults drives rapid migration to underlying aquifers. Karstic networks enhance these processes, and leakage from perched aquifers through aquitards further complicates the flow field. This combination of hydrogeological complexity and physical–chemical partitioning-sorption, volatilization, and degradation governs the long-term fate of VOCs in the system.

Importantly, the upper vadose zone remains a persistent source of VOCs, even after partial soil excavation. Without targeted in situ interventions such as soil vapor extraction or thermal treatment, PCE will continue to partition into the gas phase within the vadose zone, potentially posing long-term exposure risks in urban areas located above the contaminated perched aquifer. These findings underscore the necessity of integrated remediation strategies that address both saturated and unsaturated compartments to effectively reduce environmental and human exposure.

Beyond advancing mechanistic understanding of contaminant transport in complex vadose zones, this study provides practical guidance for site management and remediation planning. The spatial and temporal characterization of pollutant plumes, identification of high-risk hotspots, and quantification of residual contamination are essential for designing effective interventions, predicting long-term plume evolution, and mitigating ecological and public health impacts. Overall, the Jerusalem Mountains case demonstrates how comprehensive modeling, informed by sparse historical monitoring, can support evidence-based decision-making in challenging contaminated environments.

Supplementary Materials: The following supporting information can be downloaded at: https://www.mdpi.com/article/10.3390/w18060702/s1.

Author Contributions: Conceptualization, O.S., O.L., M.J.C. and H.G.; Methodology, O.S.; Software, O.S.; Validation, O.S.; Formal analysis, O.S.; Investigation, O.S.; Resources, M.J.C.; Writing—original draft, O.S.; Writing—review & editing, O.L., M.J.C. and H.G.; Visualization, O.S.; Supervision, O.L. and H.G.; Funding acquisition, O.L. and H.G. All authors have read and agreed to the published version of the manuscript.

Funding: This research was funded by the Israeli Water Authority [grant number 4501777098] and the Jewish National Fund [grant number 2860].

Data Availability Statement: The original contributions presented in this study are included in the article. Further inquiries can be directed to the corresponding author. Declaration of Generative AI and AI-Assisted Technologies in the Manuscript Preparation Process: During the preparation of this work, the authors used ChatGPT-5 (OpenAI), an AI language model, in order to improve linguistic clarity and style. After using this tool/service, the authors reviewed and edited the content as needed and take full responsibility for the content of the published article.

Conflicts of Interest: Author Caspi J. Matania was employed by the Environmental Services Company. The remaining authors declare that the research was conducted in the absence of any commercial or financial relationships that could be construed as a potential conflict of interest.

References

1. Feenstra, S.; Cherry, J.A.; Parker, B.L.; Pankow, J.F. *Dense Chlorinated Solvents and Other DNAPLs in Groundwater. History, Behavior, and Remediation*; Waterloo Press: Waterloo, ON, USA, 1996; pp. 53–88.
2. Rowe, B.L.; Toccalino, P.L.; Moran, M.J.; Zogorski, J.S.; Price, C.V. Occurrence and potential human-health relevance of volatile organic compounds in drinking water from domestic wells in the United States. *Environ. Health Perspect.* **2007**, *115*, 1539. [CrossRef] [PubMed]
3. Pandey, P.; Yadav, R. A review on volatile organic compounds (VOCs) as environmental pollutants: Fate and distribution. *Int. J. Plant Environ.* **2018**, *4*, 14–26. [CrossRef]
4. Barbash, J.; Roberts, P.V. Volatile organic chemical contamination of groundwater resources in the US. *J. Water Pollut. Control Fed.* **1986**, *58*, 343–348.
5. Rivett, M.O.; Wealthall, G.P.; Dearden, R.A.; McAlary, T.A. Review of unsaturated-zone transport and attenuation of volatile organic compound (VOC) plumes leached from shallow source zones. *J. Contam. Hydrol.* **2011**, *123*, 130–156. [CrossRef] [PubMed]
6. Gerke, H.H. Preferential flow descriptions for structured soils. *J. Plant Nutr. Soil Sci.* **2006**, *169*, 382–400. [CrossRef]
7. Pan, F.; Ye, M.; Zhu, J.; Wu, Y.S.; Hu, B.X.; Yu, Z. Incorporating layer-and local-scale heterogeneities in numerical simulation of unsaturated flow and tracer transport. *J. Contam. Hydrol.* **2009**, *103*, 194–205. [CrossRef] [PubMed]
8. Peterson, D.M.; Singletary, M.A.; Studer, J.E.; Miller, D.R. *Natural Attenuation Assessment of Multiple VOCs in a Deep Vadose Zone (No. SAND-2000-0600C)*; Sandia National Labs.: Albuquerque, NM, USA, 2000. Available online: https://inis.iaea.org/records/4sjkj-b6y22 (accessed on 11 March 2026).
9. Kirtland, B.C.; Aelion, C.M.; Stone, P.A.; Hunkeler, D. Isotopic and geochemical assessment of in situ biodegradation of chlorinated hydrocarbons. *Environ. Sci. Technol.* **2003**, *37*, 4205–4212. [CrossRef] [PubMed]
10. Oostrom, M.; Rockhold, M.L.; Thorne, P.D.; Truex, M.J.; Last, G.V.; Rohay, V.J. Carbon tetrachloride flow and transport in the subsurface of the 216-Z-9 trench at the Hanford Site. *Vadose Zone J.* **2007**, *6*, 971–984. [CrossRef]
11. Lawrence, S.J. *Description, Properties, and Degradation of Selected Volatile Organic Compounds Detected in Ground Water—A Review of Selected Literature*; Open-File Report, (2006–1338); USGS: Atlanta, GA, USA, 2006. [CrossRef]
12. Kengen, S.W.; Breidenbach, C.G.; Felske, A.; Stams, A.J.; Schraa, G.; de Vos, W.M. Reductive dechlorination of tetrachloroethene to cis-1, 2-dichloroethene by a thermophilic anaerobic enrichment culture. *Appl. Environ. Microbiol.* **1999**, *65*, 2312–2316. [CrossRef]
13. Washington, J.W. Hydrolysis rates of dissolved volatile organic compounds: Principles, temperature effects and literature review. *Groundwater* **1995**, *33*, 415–424. [CrossRef]
14. Conant, B.H.; Gillham, R.W.; Mendoza, C.A. Vapor transport of trichloroethylene in the unsaturated zone: Field and numerical modeling investigations. *Water Resour. Res.* **1996**, *32*, 9–22. [CrossRef]
15. Johnson, R.L.; McCarthy, K.A.; Perrott, M.; Mendoza, C.A. Density-driven vapor transport: Physical and numerical modelling. In *Subsurface Contamination by Immiscible Fluids*; Weyer, K.U., Ed.; Balkema: Rotterdam, The Netherlands, 1992; pp. 19–27.
16. Barber, C.; Davis, G.B.; Briegel, D.; Ward, J.K. Factors controlling the concentration of methane and other volatiles in groundwater and soil-gas around a waste site. *J. Contam. Hydrol.* **1990**, *5*, 155–169. [CrossRef]
17. Parker, J.C. Physical processes affecting natural depletion of volatile chemicals in soil and groundwater. *Vadose Zone J.* **2003**, *2*, 222–230. [CrossRef]
18. Jang, W.; Aral, M.M. Density-driven transport of volatile organic compounds and its impact on contaminated groundwater plume evolution. *Transp. Porous Media* **2007**, *67*, 353–374. [CrossRef]
19. Troldborg, M.; Binning, P.J.; Nielsen, S.; Kjeldsen, P.; Christensen, A.G. Unsaturated zone leaching models for assessing risk to groundwater of contaminated sites. *J. Contam. Hydrol.* **2009**, *105*, 28–37. [CrossRef] [PubMed]
20. Shalom, O.; Lev, O.; Livshitz, Y.; Gvirtzman, H. Groundwater Flow Modelling of a Large-Scale Thick Vadose Zone Including Two Perched Aquifers, the Jerusalem Mountains. *Hydrol. Process.* **2025**, *39*, e70216. [CrossRef]
21. Ecolog. *Roofing Begin South, A Historical Survey*; Ecolog Engineering Ltd.: Ness Ziona, Israel, 2024; 36p. Available online: https://soil-remediation.co.il/wp-content/uploads/2024/07/362033history-ver-2.pdf (accessed on 2 March 2025).

22. LDD. *Active Soil Gas Survey Findings, Begin Highway Roofing Complex, Jerusalem*; LDD Advanced Technologies, NEWPHARM Group: Petah Tikva, Israel, 2020; 260p. Available online: https://soil-remediation.co.il/project/%d7%a7%d7%99%d7%a8%d7%95%d7%99-%d7%91%d7%92%d7%99%d7%9f-%d7%a6%d7%a4%d7%95%d7%9f/ (accessed on 2 March 2025).
23. *LUDAN Final Report, Environmental Support for Rehabilitation Excavation, IMI Beit Hakerem Site*; LUDAN Environmental Technologies: Petah Tikva, Israel, 2022; 381p.
24. Diersch, H.-J. *FEFLOW—Finite Element Modeling of Flow, Mass and Heat Transport in Porous and Fractured Media*; Springer: Berlin/Heidelberg, Germany, 2014. Available online: https://link.springer.com/book/10.1007/978-3-642-38739-5?utm_medium=referral&utm_source=google_books&utm_campaign=3_pier05_buy_print&utm_content=en_08082017 (accessed on 11 March 2026).
25. Frumkin, A.; Fischhendler, I. Morphometry and distribution of isolated caves as a guide for phreatic and confined paleohydrological conditions. *Geomorphology* **2005**, *67*, 457–471. [CrossRef]
26. Frumkin, A.; Gvirtzman, H. Cross-formational rising groundwater at an artesian karstic basin: The Ayalon Saline Anomaly, Israel. *J. Hydrol.* **2006**, *318*, 316–333. [CrossRef]
27. Michelson, H. *Groundwater Contamination with Tetrachloroethylene in the Jerusalem Wells 1,3, Engineering of Water, Liquids and Irrigation*; Israel Water Industries, Internal Report; TAHAL Group: Or Yehuda, Israel, 1999; Volume 4, pp. 39–46. (In Hebrew)
28. Wealthall, G.P.; Rivett, M.O.; Dearden, R.A. A review of transport and attenuation of dissolved-phase volatile organic compounds (VOCs) in the unsaturated zone. *British Geological Survey*, 2010, 91p. (OR/10/061). Available online: https://nora.nerc.ac.uk/id/eprint/12787 (accessed on 11 March 2026).
29. Brusseau, M.L.; Carroll, K.C.; Truex, M.J.; Becker, D.J. Characterization and remediation of chlorinated volatile organic contaminants in the vadose zone. *Vadose Zone J.* **2013**, *12*, vzj2012.0137. [CrossRef] [PubMed]

Disclaimer/Publisher's Note: The statements, opinions and data contained in all publications are solely those of the individual author(s) and contributor(s) and not of MDPI and/or the editor(s). MDPI and/or the editor(s) disclaim responsibility for any injury to people or property resulting from any ideas, methods, instructions or products referred to in the content.